Master of Science Thesis in Electrical Engineering
Department of Electrical Engineering, Linköping University, 2016

Thermal modelling of voice coils in microspeakers

Johan Toverland

LINKÖPING UNIVERSITY

Master of Science Thesis in Electrical Engineering

Thermal modelling of voice coils in microspeakers

Johan Toverland

LiTH-ISY-EX--16/4975--SE

Supervisor: **Johan Dahlin**
ISY, Linköping University
Christopher Ekbom
Cirrus Logic

Examiner: **Martin Enqvist**
ISY, Linköping University

Division of Automatic Control
Department of Electrical Engineering
Linköping University
SE-581 83 Linköping, Sweden

Abstract

Microspeakers can overheat and break if not monitored and regulated. This monitoring is usually done by adding a pilot tone that introduces energy to the signal. A problem with this approach is the slow update rate of the temperature estimate. This in combination with a fast temperature rise could result in an audible regulation of the input. By simulating the voice coil temperature these problems could be mitigated. In this thesis, two existing grey box models and one novel black box model are estimated for different speakers and evaluated using different signals. The results are promising and indicate that all models can estimate the voice coil temperature with a mean error below one degree. The tests show that a correct initialization of the model is crucial. Therefore the suggestion to Cirrus Logic, who hosted this thesis project, is to combine a feedforward model with either temperature sensor data from the mobile device or a pilot tone.

Sammanfattning

Mikrohögtalare kan överhettas och gå sönder ifall temperaturen inte övervakas och regleras vid behov. Denna övervakning sker med hjälp av en pilotton som tillför energi till högtalarens insignal. Ett problem med denna lösning är att övervakningen är relativt långsam. Detta gör att en snabb temperaturökning kan ge en oönskad hörbar reglering av insignalen. Genom att modellera spolens temperatur kan detta problem hanteras. I detta examensarbete tas två fysikaliska modeller och en konfektionsmodell fram och testas på olika högtalare och signaler. Resultaten är lovande och visar att alla modeller kan skatta spoltemperaturen med ett medelfel under en grad. Utvärderingen visar att initiering av modellens starttemperatur är viktig. Därför är förslaget till Cirrus Logic att kombinera en simuleringsmodell som initieras med antingen temperatursensordata från mobilen eller med hjälp av en pilotton.

Acknowledgments

A big thank you to my examiner Martin and supervisor Johan from the university for all their help. I would also like to thank my supervisor Christopher and all other employees in Cirrus Logic's Stockholm office for their help and the nerdy lunch discussions.

Linköping, May 2016
Johan Toverland

Contents

Notation

Abbreviations are presented in the order they are found in the thesis.

Abbrevation	Meaning
V	voltage
P	power
x	displacement of membrane
T	temperature
R_{tot}	total resistance of the loudspeaker circuit
α	thermal conductivity parameter
T_{vc}	voice coil temperature
T_{a}	ambient temperature
ΔT_{vc}	change in voice coil temperature
R_{e}	voice coil resistance
P_{Re}	power dissipated in the voice coil
F_s	resonance frequency
i	current
Z	impedance response
R_1	thermal resistance of the voice coil
R_2	thermal resistance of the magnet
C_1	thermal capacitance of the voice coil
C_2	thermal capacitance of the magnet
θ	model parameters
$\epsilon(t, \theta)$	difference between the predicted and measured temperature
$\hat{y}(t \mid \theta)$	predicted model temperature
$y(t)$	measured temperature
$V(\theta)$	cost function
n	number of samples

Abbrevation	Meaning
$\widehat{\theta}$	optimal model parameters
v	velocity of the membrane
n_{a}	Model C order parameter, number of past output terms
n_{k}	Model C order parameter, input delay
N	number of partitions for Model C
β	input to the regression vector
$f(x)$	scaling function
$g(x)$	wavelet function
R	projection matrix
Q	projection matrix
K	column vector
r	mean value of the regressor vector
d	offset
a_{s}	scalar model parameters for the wavelet function
a_{w}	scalar model parameters for the wavelet function
b_{s}	scalar model parameters for the wavelet function
b_{w}	scalar model parameters for the wavelet function
c_{s}	row vector for the wavelet function
c_{w}	row vector for the wavelet function
N_{r}	number of regressors
$U(k,l)$	energy in the frequency domain
k	lower frequency limit
l	upper frequency limit
f	frequency
σ	vector used when creating the regressor input vector to Model C
ς	vector used when creating the regressor input vector to Model C
N_{f}	length of the frequency vector
a	curve function parameter
$\bar{\beta}(t)$	mean energy of all partitions
L	curve function deciding partition length of Model C
χ	a normalised length vector
$R_0(T_{\mathrm{a}})$	the voice coil resistance at the ambient temperature
ϵ_{val}	mean absolute error for the validation data
ϵ_{est}	mean absolute error for the estimation data
ϵ_{max}	maximum absolute error for the validation data
ϵ_{init}	mean absolute error for the chosen model parameters
$\epsilon_{\mathrm{changed}}$	mean absolute error for the changed model parameters

1 Introduction

A microspeaker is a small speaker that primarily is used in smart phones and tablets. The temperature of the voice coil in these speakers can rise rapidly during operation, causing damage to the components of the microspeaker and even function failure. To avoid this, it is important to measure the temperature of the voice coil so that the input to the microspeaker can be regulated to keep the temperature within its operational range. One way to achieve this is to add a low frequency *pilot tone* and measure the impedance over the speaker circuit. The voice coil temperature can be estimated from the impedance measurement, since the resistance of the metal in the voice coil is temperature dependent. This method has two drawbacks: the pilot tone adds unnecessary energy which heat up the voice coil and the observation rate is slow in the regulation system and in combination with a fast temperature rise this can lead to an unwanted audible regulation of the input signal. This thesis investigates three different thermal models that are supposed to predict the voice coil temperature instead of measuring it.

1.1 Background and motivation

The smart phone market has grown for several years and is now a multi-billion industry with several large businesses competing for market shares [Marketline, 2015]. This competition has resulted in products that demand a high level of technology at a low cost, such as faster mobile processors and high resolution screens. A recent focus in these devices is the sound quality and being able to play as loud as possible. This has been achieved by using a boosted amplifier to increase the signal to the speaker, leading to a larger input power. However, this can cause overheating since these small speakers often have a lower power rating than the amplifier.

This problem is solved by monitoring the voice coil temperature and regulating the input signal before the voice coil starts to overheat. For this to work, the voice coil temperature has to be measured. As mentioned above, one method to find the voice coil temperature would be to add a pilot tone and measure the momentary impedance. Another similar method is to measure the impedance without a pilot tone. The impedance is then measured over a frequency interval where there usually is frequency content. One disadvantage with this method is that the measurements can get noisy if there is limited frequency content in the measured interval. The second method has the same drawback as the first method concerning the slow observation rate in the regulation system.

The issues created by measuring the voice coil temperature could be mitigated if a feedforward model could be found, which is able to estimate the temperature based on the speaker input signal. This could result in cheaper loudspeaker circuits if the model performs well enough and removes the need for the measurement of the impedance.

1.2 Related works

The usual way of modelling loudspeakers is by dividing the speaker into an electromechanical model and a thermal model. Figure 1.1 shows that the electromechanical model is temperature dependent and how the thermal model depends on the electromechanical model for its input, see Klippel [2004] for more information.

1.2.1 Electromechanical models

The electromechanical model describes the electromechanical characteristics of a loudspeaker and was first introduced in the 1970s by Small [1972] and Thiele [1971]. It was the first successful model of the operation of a loudspeaker and this linear model was later developed into the well-known Thiele/Small parameters. This model has later been improved to include nonlinearities in the loudspeaker function, see Andersson [2008]. According to Klippel [2004], there are some nonlinearities in the electromechanical model that could affect the thermal model. For example the power over a cold voice coil is several times higher for lower frequencies than a linear electromechanical model can explain. This could alter the results of the thermal model in a negative way, since the calculated power is used as an input to the thermal model.

An increasing speaker temperature alters the Q-factor of the loudspeaker, which changes the appearance of the transfer function of the electromechanical model. According to Andersson [2008], the Q-factor is defined as a ratio of the voice coil resistance to the motional reactance of the resonance frequency of the loudspeaker membrane. Using this characteristics, Pedersen and Rubak [2007] made

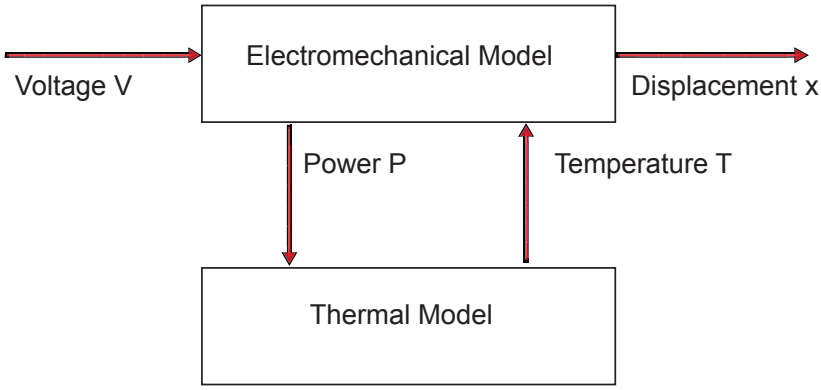

Figure 1.1: *A diagram showing the relationship between the thermal and the electromechanical model. The temperature T is calculated in the thermal model from the power P, which is calculated from the input voltage V and the temperature T in the electromechanical model. Here, the output x denotes the displacement of the loudspeaker membrane.*

use of FIR filters to find the electromechanical model parameters during operation. Furthermore, they mention that this could be used to estimate the voice coil temperature. Andersson [2008] used this approach but adds an adaptive filter to estimate the voice coil temperature. However, the results were not conclusive and measurement errors were held accountable. These methods require both voltage and current measurements, which are not always available in practice.

1.2.2 Thermal models

The thermal model describes how the input power is converted to heat and how that heat is transfered between the speaker components [Henricksen, 1986]. In this model, the heat transfer processes are modelled by thermal equivalent resistances and capacitances. This kind of model is known as a lumped-element model, see Chapman [1998] for more information.

The model is often simplified to two RC submodels, where all parallel heat transfer mechanisms are lumped together as one thermal resistor and capacitor for the voice coil and the magnet [Button, 1992, Zuccatti, 1990], respectively. Behler and Bernhard [1998] expanded this model with an extra RC submodel for the cabinet of the speaker and proposed a method to estimate the parameters of the model. Chapman [1998] improved the model further by moving out the capaci-

tance from the RC submodel. This results in that simulations are accurate with an error between 0.7 and 2°C depending on the type of speaker.

According to Klippel [2004], the previously mentioned linear models do not account for the forced cooling due to the movement of the speaker membrane. A nonlinear lumped elements model, which includes this and some additional effects was proposed and tested by Klippel [2004]. In the same year, Blasizzo [2004] published a model where the forced convection and eddy currents were considered.

1.3 Contributions and results

In order to examine if a feedforward model is able to estimate the voice coil temperature, three different models will be compared and analysed. The common approach in earlier work in thermal modelling has been to draw conclusions from how different thermal processes affect the speaker and based on those observations create a thermal equivalent circuit model. In this thesis, two of these grey box models will be compared with a nonlinear black box model. This approach differs slightly from most well-known papers on the subject, since the usual way is to use physics-based models. Another difference is the focus on microloudspeakers, because most studies on thermal modelling have been done on regular loudspeakers. The following models have been implemented in this thesis.

Model A is a linear grey box model similar to the one proposed by Chapman [1998] and Model B is a nonlinear grey box model with the structure suggested by Klippel [2004]. Both these models are supposed to give an accurate description of the voice coil temperature. The black box model, Model C, is a NARX model where the input vector is the energy of the voltage in different frequency intervals. In an ordinary music signal the energy is mostly concentrated at the lower frequencies. Therefore, these frequency intervals will have a varying size in accordance with this behaviour.

Finding the model parameters will be done in two steps. First temperature data from experiments will be collected using the pilot tone approach. The model parameters are then estimated using the collected temperature data and system identification. This is done by minimizing the error between the experimental data and the model prediction of the voice coil temperature. Comparison of the three models will be done with different kinds of music and speech signals. Music is considered the main use of a speaker and the estimation of the model parameters will therefore be made on music.

Some limitations were considered such that the Master's thesis project could fit the time schedule. The thesis will focus on the comparison of thermal models. Therefore no electromechanical model will be implemented. The input to the thermal model will instead be calculated using the current and the temperature

dependent voice coil resistance. Here, calculations will be done off-line with no defined limitation of the computational power. In a commercial product this will have to be further examined since the computational power is limited in the devices using microspeakers. Therefore the thermal models will not be implemented in a commercial device during the time of the Master's thesis. The thermal effect caused by eddy currents in the speaker where power bypasses the voice coil and directly heats the magnet will not be considered.

1.4 Cirrus Logic Sweden AB

Opalum was founded by Pär G. Risberg in 2007, an alumni from the Applied Physics and Electrical Engineering programme at Linköping University. The company's sound processing technology made it possible to create thin active loudspeakers with high sound qualities that otherwise were reserved for larger loudspeakers. After creating their flagship speakers Opalum started to look upon the smart phone market and how to improve the sound and durability of microspeakers in smart phones. This resulted in both speaker protection, distortion reduction and other improvement algorithms for microspeakers.

In 2015, the American sound company Cirrus Logic acquired the Opalum sound technology and their software office in Stockholm. Cirrus Logic was founded 1984 and provides both software and hardware solutions for audio components used in smart phones, tablets and other audio applications. The company is now based in Austin, Texas and has offices in Europe and Asia with around 1,100 employees in total. Cirrus Logic's Stockholm office is now working on a consumer platform for their software while at the same time creating new algorithms for speaker protection and better sound quality.

1.5 Thesis outline

In Chapter 2 the function and the components of the microspeaker are explained. A short introduction is given about thermal effects and processes and how they affect speakers. This is concluded with highlighting nonlinear thermal effects that have been observed in speakers.

In Chapter 3, the three different models are introduced. This is done by giving a theoretical background of the models and discussing how the models can be implemented. The concepts of grey box modelling, lumped elements models and black box modelling will be touched upon.

Chapter 4 shows the results of the three different models for estimation and validation data. The models' sensitivity are analysed by perturbing the model parameters. Model behaviour is analysed at different ambient temperatures and the model initialization is discussed.

In Chapter 5 a short summary of the result is given and a comparative discussion about the performance is made about the different thermal models. This discussion will result in some ideas how to continue with these models and how they could be used by Cirrus Logic. After this, some general conclusions about the accomplishments of the thesis are given.

2

Microspeakers and their properties

This chapter provides an explanation of how a microspeaker works and clarifies the function of the speaker components. Different thermal processes that appear in loudspeakers are discussed and their effects according to previous research and experiments are presented.

2.1 The microspeaker components and function

The microspeaker (or micro-loudspeaker) is according to Bright [2002] a small and thin loudspeaker that is often used in smaller electronic devices such as tablets and smartphones. These microspeakers are very similar to larger loudspeakers and the main difference is the size. A cross section of the microspeaker and its components is presented in Figure 2.1.

A microspeaker is a transducer that creates sound waves from electrical power. The core concept is that a current runs through a voice coil that is situated in a magnetic field. This creates a force that pushes the diaphragm (also called a membrane), which moves the air around the speaker and creates sound pressure. The membrane is also fixed to the frame and there is a magnetic circuit that directs the magnetic field from the speaker magnet [Bright, 2002].

This transduction from voltage to sound pressure is inefficient. Only about 5% of the energy is converted to sound. The remaining energy becomes heat that spreads through the components in the speaker. Speaker failure can therefore occur as too much heat leads to degradation of the materials and the adhesives inside the microspeaker [Henricksen, 1986, Button, 1992].

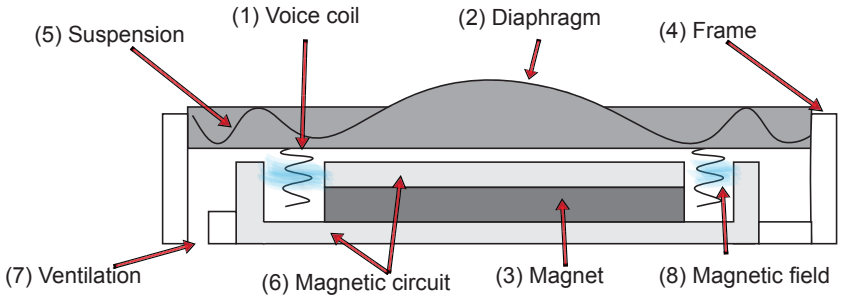

Figure 2.1: *A cross-section of a microspeaker.*

2.2 Thermal properties

When heat is generated in a speaker it spreads between the different elements of the loudspeaker according to the five thermal processes, conduction, radiation, natural and forced convection and thermal storage [Henricksen, 1986].

Conduction transfers heat from a hot source to a colder sink through a physical path. In the microspeaker, heat is conducted from the voice coil to the adjacent parts during operation. Behler and Bernhard [1998] explain that the voice coil is the largest source of heat in the speaker. This heat is caused by the resistance of the voice coil when electrical power surges through it. The conduction takes place in the air gap between the voice coil, the magnet and the magnet circuitry. The heat is then dissipated to the ambient air through the frame, the magnet or the membrane.

Heat transfer from radiation occurs when a body loses energy through electromagnetic emission. This effect increases with higher temperature. However, this effect is minor below $150°C$ according to Henricksen [1986] and Zuccatti [1990]. The working temperature of a microloudspeaker is below $100°C$. Therefore, the radiation effect in microspeakers is insignificant.

At lower frequencies the loudspeaker membrane motion forces air and heat from the speaker to the ambiance through the ventilation holes. Hence, the membrane acts as a bellow and pumps air in and out of the speaker. This is called forced convection and can be seen as a frequency dependent cooling factor [Klippel, 2004]. The cooling factor is the decrease in temperature that occurs because of the forced convection. Henricksen [1986] detects a $5°C$ cooling factor for a $100°C$ warm voice coil in a subwoofer speaker. He also notices that the cooling factor increases with an increasing membrane velocity. There is also natural convection

which is the airflow created when hot air rises. Klippel [2004] concludes that in speakers this effect depends on the membrane position since this changes the amount of air surrounding the voice coil.

Thermal storage is the thermal process occurring when an object gets warmer. This means that the temperature of the object will rise when heat is added. The heat will be stored in the object if a heat transfer effect does not dissipate it. In the microspeaker the main components of interest are the voice coil and the magnet. The magnet is interesting because it is the largest thermal reservoir with the capacity to store a lot of thermal energy and dissipating it slowly. The voice coil is interesting because it has a small capacity for storage of thermal energy and therefore dissipates it faster.

The ability of the loudspeaker element to shed and gain heat is called the element's thermal resistance. This thermal resistance describes the change in temperature when heat is added to the element. It is often calculated as °C / W [Henricksen, 1986].

Power compression is a temperature dependent process but not a thermal one. When a constant voltage is applied to a micro-speaker, the temperature will start to rise and the input power will be reduced with the increased temperature. The end result is that the power compression becomes an extra safety against overheating. As can be seen in Figure 2.2, the change in temperature ΔT_{vc} is smaller at higher temperatures. Therefore, the input power must be larger to result in the same temperature change when the voice coil is warmer. The input power P is calculated as

$$P = R_e(T_{\text{vc}})i^2, \tag{2.1}$$

where, $R_{\text{e}}(T_{\text{vc}})$ denotes the temperature dependent voice coil resistance and i denotes the current applied to the speaker. According to Henricksen [1986], the power compression effect is audible when a cold speaker is supplied with a high power input signal. The volume will then decrease over time as the speaker gets warmer.

2.3 Nonlinear thermal effects

Klippel [2004] calculates the total thermal resistance of the speaker as

$$R_{\text{tot}} = \Delta T_{\text{vc}} / P_{\text{Re}}, \tag{2.2}$$

where P_{Re} denotes the power dissipated in the voice coil and ΔT_{vc} is the change in voice coil temperature. He concludes that R_{tot} varies up to 60% depending on the input signal when comparing contemporary music with high bass content against an a cappella song. The high bass content in the former piece leads to cooling of the voice coil through forced convection. This forced convection depends on the velocity of the speaker membrane or rather how much air that is moved by the membrane. A higher velocity therefore gives a higher airflow and

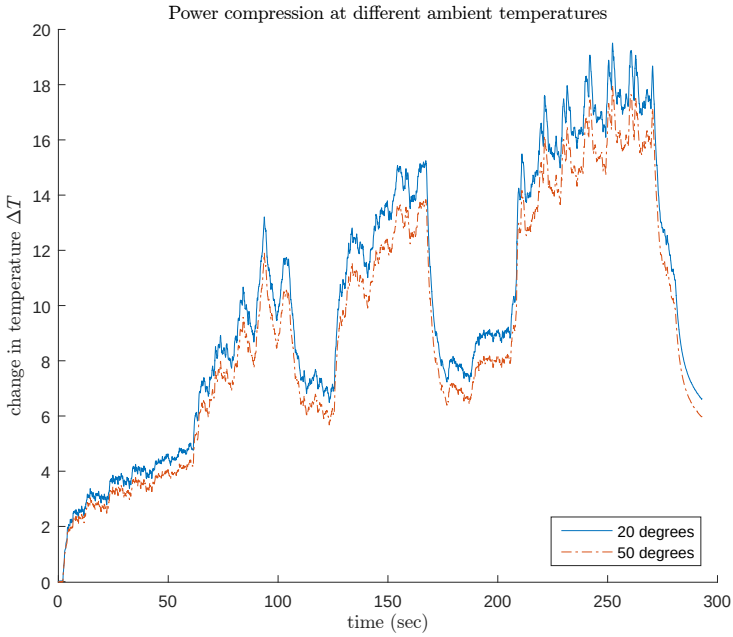

Figure 2.2: *The change in temperature when applying the same input signal for two different ambient temperatures: 20 degrees (blue solid) and 50 degrees (orange dashed).*

more cooling of the voice coil. As mentioned in Section 2.2 the forced convection is frequency-dependent. The velocity of the speaker membrane is highest when the frequency of the input signal is close to the resonance frequency F_s, as can be seen in Figure 2.3. An experiment was carried out to show the cooling down effect of the forced convection, see Figure 2.4. This is something that is not considered in traditional linear thermal modelling of loudspeakers.

The natural convection can be decreased because of amplitude compression of velocity and membrane displacement. The excursion of the membrane gets smaller at higher frequencies as can be seen in Figure 2.5. However, Klippel [2004] considered the effect of this decreased convection as negligible in comparison to the forced convection.

Another nonlinear effect is that the input power to the thermal model is dependent on the impedance response of the loudspeaker. When calculating the current, which has to be done if the current can not be observed and measured, in the power equation (2.1) the impedance response is used in the following way

$$i(t, f, T) = V(t)\frac{1}{Z(f, T)}. \tag{2.3}$$

Here, $i(t, f, T)$ denotes the current, $V(t)$ denotes the input voltage and $Z(f, T)$ denotes the impedance response [Chapman, 1998]. This response can also vary because of non-linearities in the driver [Klippel, 2004]. Since, the input power is calculated by the electromechanical model as can be seen in Figure 1.1, this is beyond the scope of this thesis and the current is instead measured.

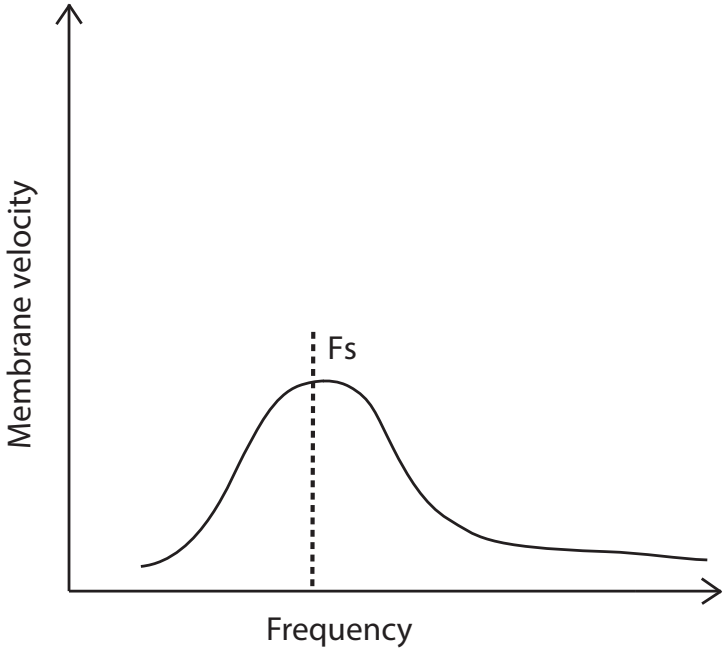

Figure 2.3: *The generalised shape of the diaphragm velocity as a function of frequency. Here, F_s denotes the resonance frequency of the driver in the loudspeaker.*

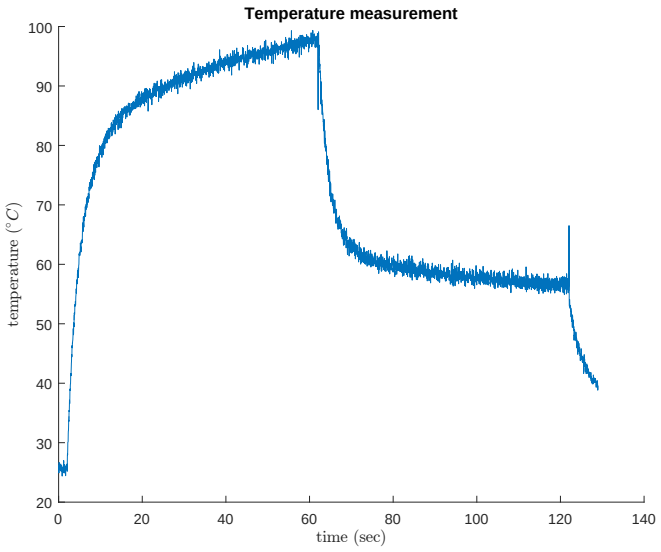

Figure 2.4: *The measured temperature shows the effect of the forced convection. The input during the first 60 seconds is a 4,000 Hz sine wave, resulting in small excursions of the membrane. After 60 seconds another sine wave was added to the original tone with a frequency close to the resonance frequency. This results in a high membrane excursion and a cooling effect on the voice coil.*

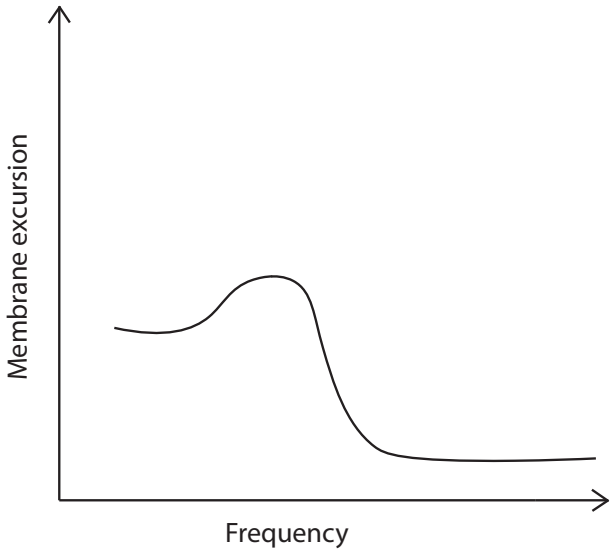

Figure 2.5: *The generalised shape of the diaphragm excursion as a function of frequency.*

3

Thermal modelling

This chapter presents the implementation and estimation of three different thermal models: lumped element models, grey box models and black box models.

3.1 Grey box modelling and lumped element models

According to Ljung and Glad [2004], there are two basic principles of how to model systems. The first principle is to create subsystems using the knowledge about the system and natural laws, such as Kirchhoff's and Ohm's laws. The second basic principle is to use identification to select the model parameters using observations from the system. The concept of grey box modelling make use of both these principles.

Ljung and Glad [2004] also mention the analogies between different physical domains. For example, capacitance in a electrical system is similar to the thermal storage in a thermal system. The thermal analogy for electrical resistance is heat resistance or thermal resistance as mentioned in Section 2.2. The idea that different physical domains have systematic similarities results in the conclusion that a thermal system can be treated as an electrical system with different variables and parameters. Henricksen [1986] made use of this idea to model the thermal processes in a loudspeaker as a thermal equivalent of an electrical circuit. This kind of model is called a *lumped element model* [Chapman, 1998].

Three models, Models A, B and C are investigated in this thesis. Both Models A and B are lumped element models but also grey box models, as they are built upon physical relations. Model A is a linear model and Model B is a linear parameter-varying Model. This makes model B nonlinear across time, but linear at every singular time instance.

3.1.1 Model A

The linear model in Figure 3.1 was created from the circuit suggested by Chapman [1998]. Here, the thermal resistance denoted by $R1$ and the thermal capacitance denoted by $C1$ are the thermal elements of the voice coil element in the speaker. The thermal resistance for the magnet is denoted by $R2$ and the capacitance is denoted by $C2$. The thermal equivalent of the current is the power denoted by P and the equivalent change in voltage is the change in temperature. The change in voice coil temperature denoted by ΔT_{vc} is given by $\Delta T_{\mathrm{vc}} = T_{\mathrm{vc}} - T_{\mathrm{a}}$. Here T_{vc} denotes the temperature of the voice coil and T_a denotes the ambient temperature around the speaker. Analogously, ΔT_{m} denotes the change in temperature for the magnet.

This model is based upon a earlier thermal model of the voice coil temperature described by Henricksen [1986], Zuccatti [1990] and Button [1992]. Both models are very similar, the difference is the positioning of the resistances and the capacitances as shown in Figure 3.2.

The s-plane transfer function for the change in voice coil temperature ΔT_{vc} for Model A is given by

$$\Delta T_{\mathrm{vc}} = \frac{R_1 + R_2 + s(R_1 R_2 C_2)}{1 + s(R_1 C_1 + R_2 C_1 + R_2 C_2) + s^2(R_1 C_1 R_2 C_2)} P. \tag{3.1}$$

The implementation of Model A is done by mapping the s-plane transfer function from the Laplace domain to the discrete equivalent z-plane. This mapping is done using Tustin's method. A digital filter is created from the mapped transfer function. The output of this filter is the simulated temperature $\hat{y}(t \mid \theta)$, were θ are the model parameters, R_1, C_1, R_2 and C_2. The input is the calculated power P in (2.1). This leaves us with an output error problem given by

$$\epsilon(t, \theta) = y(t) - \hat{y}(t \mid \theta), \tag{3.2}$$

where $\epsilon(t, \theta)$ denotes the difference between the measured temperature $y(t)$ and the simulated temperature $\hat{y}(t \mid \theta)$. Let us introduce a cost function given by

$$V(\theta) = \frac{1}{n} \sum_{t=1}^{n} \epsilon^2, \tag{3.3}$$

where n denotes the number of samples in the observation. The optimal model parameters $\widehat{\theta}$ can be estimated by minimizing the cost function using a nonlinear solver. These parameters are then used when validating the model. With optimal model parameters the model should be able to simulate the system's behaviour.

3.1.2 Model B

Model B, which is a nonlinear model, was created from the circuit shown in Figure 3.3. As can be seen this is very similar to the linear model except for the

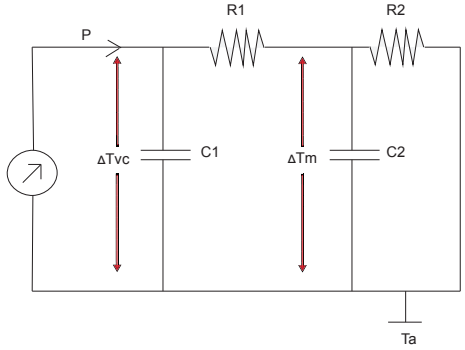

Figure 3.1: *The linear thermal circuit model used for Model A [Chapman, 1998]. The power P will flow into the thermal capacitance $C1$ of the voice coil. With an increasing temperature over the voice coil, the power will start to flow to the magnet thermal capacitance $C2$ through the voice coil thermal resistance $R1$. When the magnet starts to heat up, the power left will flow through the magnet thermal resistance $R2$ to the ambiance T_a.*

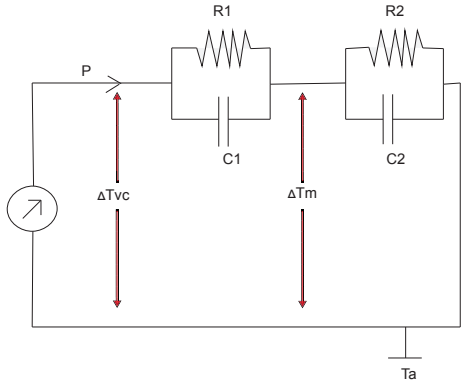

Figure 3.2: *Linear thermal circuit model suggested by Henricksen [1986], Zuccatti [1990] and Button [1992]. Comparing this circuit with Figure 3.1, the different positioning of $C1$ and $C2$ is evident.*

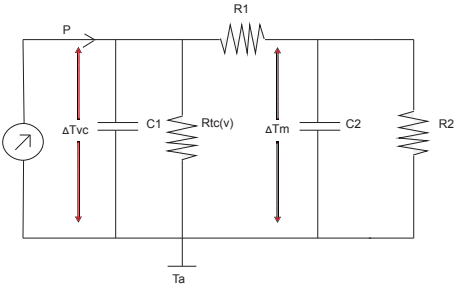

Figure 3.3: *The nonlinear thermal circuit model used for Model B [Klippel, 2004]. The diffence between this model and Chapman [1998] is the forced convection variable $R_{tc}(v)$. This thermal resistance changes depending on the velocity of the membrane and therefore makes the model nonlinear.*

component $R_{tc}(v)$. This component is supposed to capture the forced convection of the speaker and is calculated by

$$R_{\mathrm{tc}}(v) = \frac{1}{v\phi}. \tag{3.4}$$

Here, v denotes the root mean squared value of the velocity of the speaker membrane and ϕ denotes a constant parameter. The length of the root mean square window was 5512 samples or $0.125s$, the same as the downsampled temperature observation. The velocity of the membrane v is calculated from the measured excursion of the membrane. To reduce measurement noise in the excursion signal, a short moving average filter was applied in a preprocessing step. The implementation of Model B is different from Model A. Instead of using a filter and the transfer function, the circuit is modelled directly using Simulink™. This means that the thermal circuit in Figure 3.3 was implemented as a circuit in the Simulink™ environment and the result is shown in Figure 3.4. This model outputs the simulated temperature $\hat{y}(t \mid \theta)$ with the model parameters $R1$, $C1$, $R2$, $C2$ and the forced convection parameter ϕ. The estimation of the model parameters is done in the same way as for Model A, by minimising (3.3). The model parameters θ in Model A and Model B represent the same physical relations with the exception of the extra model parameter ϕ which does not exist in Model A.

3.2 Black box modelling

Black box models describe only the relation between the input and output of a system. This is done by observing the system and optimising the parameters of a generalised model to fit the system. This approach differs from grey box models because it does not use the physical characteristics of the system. However,

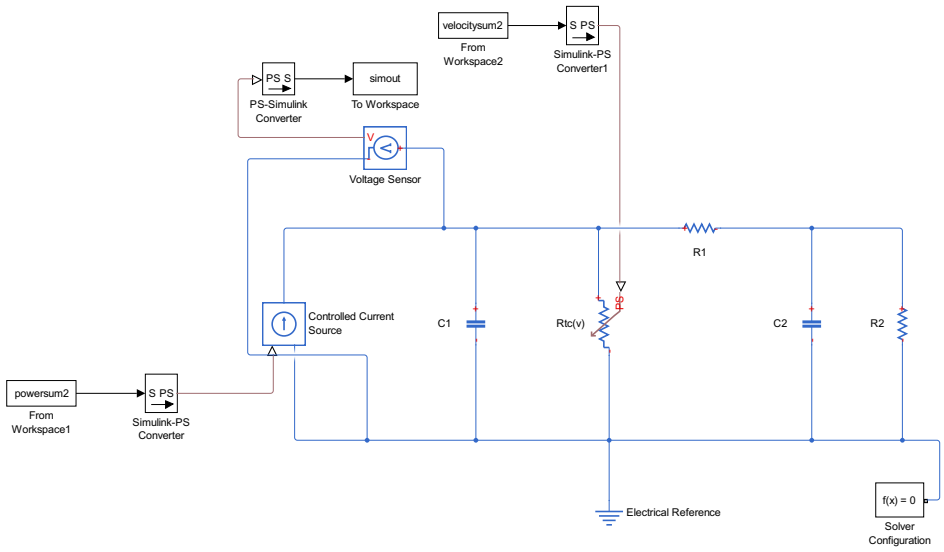

Figure 3.4: *The Simulink™ implementation of Model B.*

according to Ljung and Glad [2004] the generalised models can be adjusted such that information about the system characteristics can be utilised.

3.2.1 Model C

Model C is a nonlinear autoregressive model with exogenous input and it is presented in Figure 3.5. The idea behind this model is that the temperature change of the voice coil depends on the frequency content of the input, which can be described by

$$\hat{y}(t) = F(\varphi(t)) \tag{3.5}$$

where,

$$\varphi(t) = [\hat{y}(t-1), \ldots, \hat{y}(t-n_a), \beta(t-n_k, 1), \beta(t-n_k, 2), \ldots, \beta(t-n_k, N)]. \tag{3.6}$$

Here, $\hat{y}(t)$ denotes the simulated temperature of the voice coil $y(t)$. Furthermore, $\varphi(t)$ denotes the regression vector determined by the orders n_a, n_k and the number of partitions N. The input to the regression vector is denoted by β and will be explained in detail later. The remaining part of the regression vector is already simulated values $\hat{y}(t-1), \ldots, \hat{y}(t-n_a)$. The model nonlinearity is defined as

$$\begin{aligned} F(\varphi(t)) = (\varphi(t) - r)RK + a_s f(b_s((\varphi(t) - r)Q - c_s)) \\ + a_w g(b_w((\varphi(t) - r)Q - c_w)) + d \end{aligned} \tag{3.7}$$

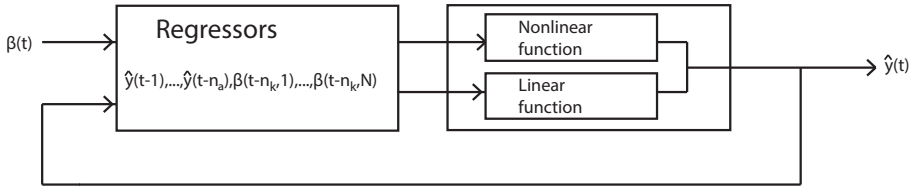

Figure 3.5: *A representation of Model C where the input β is the energy in different frequency ranges and $\hat{y}(t)$ is the predicted temperature. The nonlinearity is a wavelet function described in* (3.7) *and the linear function is an ARX model.*

where

$$\begin{aligned} f(x) &= e^{0.5xx^\top} \\ g(x) &= (N_r - xx^\top)e^{0.5xx^\top}. \end{aligned} \tag{3.8}$$

Here, $f(x)$ denotes a scaling function, $g(x)$ denotes the wavelet function, R and Q denote projection matrices composed using principal component analysis of the estimation data. Furthermore, K denotes a column vector, r denotes the mean value of the regressor vector calculated from the estimated data, d denotes an offset and is together with a_s, a_w, b_s, and b_w scalar model parameters and c_s and c_w denote row vectors. Finally, N_r denotes the number of regressors.

When the model was estimated, a prediction problem was solved instead of a simulation problem. The difference is that the earlier temperature values in the dataset are known to the solver and not predicted. This means that when estimating the model, the regression vector contains the observed temperature values and the input: $y(t-1), \ldots, y(t-n_a), \beta(t-n_k, 1), \beta(t-n_k, 2), \ldots, \beta(t-n_k, N)$ and with this information $\hat{y}(t)$ is predicted. The model parameters are optimised using the nonlinear least squares method.

The input to this model is the voltage over the speaker $u(t)$ after pre-processing. Here, the voltage input is split into short time intervals that are 5512 samples long or 0.125s long when using a sample frequency of 44100. The mean energy of the input in a particular frequency interval is given by the discrete Fourier transform and Parseval's theorem as

$$U(k,l) = \frac{1}{N_f - (k+l)} \sum_{k}^{N_f-1-l} |\mathcal{F}(u(t))|^2, \tag{3.9}$$

where k denotes the lower frequency limit, l denotes the upper frequency limit, $\mathcal{F}$ denotes the discrete Fourier transform and N_f is the length of the frequency

vector. The data calculated by the Fourier transform is the voltage input $u(t)$ for each short time interval. The energy $U(k, l)$ is partitioned N times resulting in the regressors $\beta(t - n_k, 1), \ldots, \beta(t - n_k, N)$, where each partition quantifies the mean energy of a specific frequency range decided by k and l. Partitions are made shorter at low frequencies and then increase in size exponentially because the energy in music is often centered around low frequencies.

This is done by creating a vector σ with N values. These values are set to $1/N$. Another vector ς is calculated by multiplying

$$\varsigma = \sigma L(\chi) \tag{3.10}$$

where,

$$L(\chi) = (a^{\chi} - 1)/(a - 1) \tag{3.11}$$

and

$$\chi = 1/N, 2/N, \ldots, N/N. \tag{3.12}$$

Here, a denotes the curve parameter and χ denotes a vector with length N. The curve L is seen in Figure 3.6. ς is then normalised by dividing the vector values with the sum of all vector values. After this step the ς vector is multiplied with the length of the frequency axis given by the discrete Fourier transform. The values in this new vector are rounded of to the closest integer. Some manipulation is now made ensuring that the combined length of the partitions matches the length of the frequency axis. First a check is made if the combined length of the partitions is shorter or longer than the Nyquist frequency and depending on that outcome, one is added to or removed from one of the partitions. That partition is chosen based upon where one added or removed sample makes the least difference from the vector before it was discretised. After this step, all partitions are checked if they have a zero value. If that is the case, the partition with the largest value is decreased by one and this value is added to the partition with the zero value. All this creates a vector that defines the parameters k and l. That in turn defines the frequencies that each partition quantifies the mean energy over. When the partitions vector is created, $\beta(t - n_k, 1), \ldots, \beta(t - n_k, N)$ can be calculated for an input signal by calculating the mean energy over each partition and its specific frequency range. The different lengths of the partitions can be seen in Figure 3.7.

The custom partition length is decided by choosing the number of partitions N and a curve parameter a. These parameters are optimised with the help of an input signal to the loudspeaker. Pink noise was chosen as an input signal because it excites all frequencies up to the Nyquist frequency and it is similar to music in its construction. This noise is created by filtering white noise with a −3dB slope low-pass filter. Then, a nonlinear solver is used to calculate the optimal value for the parameter a for those choices by minimizing the cost function V given by

$$V = \frac{1}{N} \sum_{t=1}^{n} \sum_{k=1}^{N} |\beta(t, k) - \bar{\beta}(t)|^2 \tag{3.13}$$

and

$$\bar{\beta}(t) = \frac{1}{N_p} \sum_{k=1}^{N} \beta(t, k). \tag{3.14}$$

Where, $\bar{\beta}(t)$ is the mean energy over all partitions. When the optimal value of a has been chosen by the solver the input vector $\beta(t - n_k, 1), \ldots, \beta(t - n_k, N)$ can be calculated for any input signal.

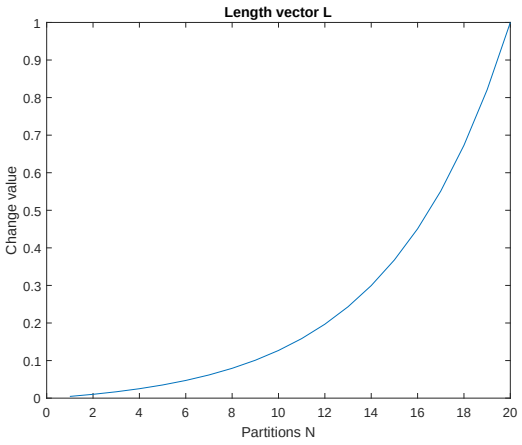

Figure 3.6: *The length curve L for the parameter value $a = 47.3$. This curve decides the specific frequency range for each partition $\beta(t - n_k, N)$. The change value is the value of the length curve and decides the length of the different partitions.*

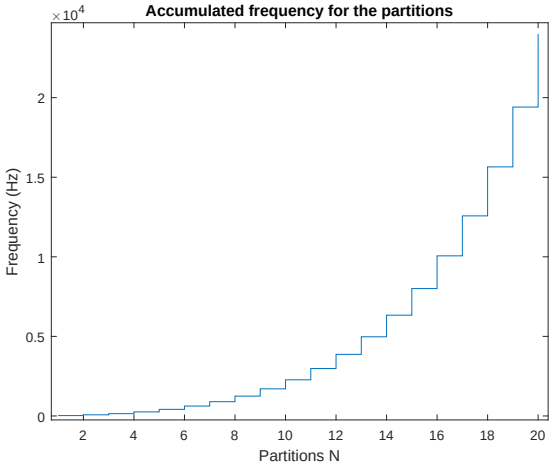

Figure 3.7: *The accumulated partition length for $a = 47.3$. Each partition quantifies the energy over a specific frequency range. The partitions are shorter in the lower frequencies and this is because most of the energy in music is situated in those frequencies.*

4

Comparing and validating thermal models

This chapter presents the performance of the three models and some details about the experimental setup are discussed. A sensitivity analysis is made to see how the ambient temperature and parameter changes alter the performance of the models.

4.1 Experimental setup and pilot tone

Experimental temperature data was measured using the pilot tone approach and the equipment listed in Appendix 5. In the pilot tone approach, the resistance of the voice coil is calculated by measuring the voltage and current in a small frequency area determined by the pilot tone. For every period of the pilot tone the root mean square value of the current and the voltage is used to calculate the resistance of that time period. The temperature can be estimated by using the fact that the voice coil resistance is temperature dependent,

$$R_{\mathrm{e}}(T_{\mathrm{vc}}) = R_0(T_{\mathrm{a}})(1 + \alpha \cdot \Delta T_{\mathrm{vc}}). \tag{4.1}$$

Here, $R_{\mathrm{e}}(T_{\mathrm{vc}})$ denotes the temperature dependent resistance of the voice coil, $R_0(T_{\mathrm{a}})$ denotes the resistance at the ambient temperature T_{a}, α denotes the temperature coefficient of the voice coil material and ΔT_{vc} denotes the difference in temperature from the ambiance. The thermal parameters $R_0(T_{\mathrm{a}})$ and α were estimated by heating the microspeakers to different temperatures and measuring the resulting resistance. With this information, the parameters of the linear function were calculated by a polynomial fitting function [Polyfit function]. Three speakers were tested in the sensitivity analysis, two smaller microspeakers (Speaker 1 and 2) and one slightly larger (Speaker 3), see Figure 4.1. The thermal parameters for the three speakers are presented in Table 4.1. The frequency of the pilot tone was chosen so the phase shift between the current and the voltage was

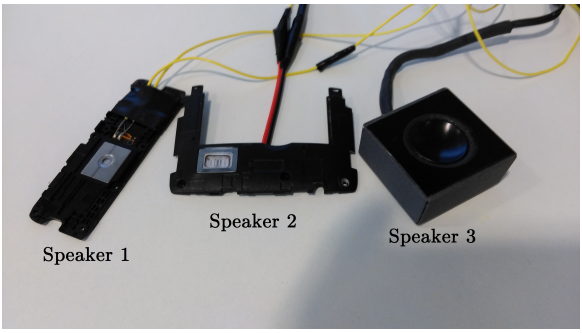

Figure 4.1: *The three different speakers that were used in the sensitivity analysis. Speaker 1 was used for the remainder of the results.*

close to zero. For Speakers 1 and 2, a 40Hz sine waves was selected and a 10Hz sine wave was selected for the third Speaker. These sine wave were implemented with −30dB smaller amplitude than the maximum amplitude of the signal. The idea was that this should result in a minimal impact on the temperature of the speaker by adding as little energy as possible. Another reason why the pilot tone was chosen at 40Hz is that the membrane of a microspeaker does not move for frequencies below 100Hz. Therefore no forced convection should be created by this added tone. The temperature of the voice coil was estimated for every period of the pilot tone.

The input power is calculated by measuring the current and using the temperature dependent resistance of the voice coil (4.1). The power is then calculated as

$$P = R_e(T_{\text{vc}})i^2. \tag{4.2}$$

The temperature value in T_{vc} in the power equation is initialized using the first observed temperature value. After the initialization the value is calculated by the thermal models.

A laser was used to measure the excursion of the speaker membrane. For Speakers 2 and 3 this was straightforward but the cabinet surrounding speaker 1 was closed and the membrane therefore not visible. Instead a custom-made speaker cabinet with a small hole in the cabinet was used, so that the membrane was visible and measurable, see Figure 4.1. The velocity of the membrane was calculated using the excursion data. This velocity signal is used as an input to Model B and its forced convection resistance $R_{\text{tc}}(v)$. A 10 sample long mean average filter was applied to the velocity signal because it was noisy. After this a root mean square window with a length of 5512 samples was applied to the velocity signal.

4.1.1 Downsampling

Most of the experimental data was collected with a sample rate of 48kHz. The data was downsampled to a frequency of 8Hz since the thermal system is significantly slower. When downsampling, an anti-alias filter was used to minimize aliasing effects. The mean of the power and the membrane velocity were calculated for the previous $48,000/8 = 6,000$ samples.

4.2 Comparison method

Three kinds of input signals were used when comparing Models A, B and C. The first kind was contemporary music with a large amount of bass. This *modern* music should excite the membrane and give a high membrane velocity resulting in forced convection. The second kind was jazz and classical music. Here, the bass is not so dominating and there is a larger amount of higher frequencies compared with contemporary music. Speech was the last kind of input signal. This signal has a lot of pauses but also high excursion since speech is similar to pulse trains. The speech signals were recorded from video blogs and talk shows. Estimation of the three models was done using two songs from the contemporary category and two songs from the classical/ jazz category. Validation of the models was done on all three kinds of input signals. The mean model error, see (3.2), will be the basis of the comparison between the different models and the different kinds of input signals. When calculating the mean model error for several songs, the total sum of the absolute error for all songs is divided by the total length of all songs. Other important metrics for comparison are the largest error, the bias and the variance of the error both with respect to time and temperature.

4.3 Model comparison

Table 4.2 summarises the different input signals that have been used for the estimation and the validation. Songs number 1, 3, 5 and 6 were used for estimation for all models. The remaining songs in the different music categories are used for validation and the main focus of the estimation was to create an accurate model primarily for different kinds of music. Therefore, there are no speech signals among the estimation datasets as they could affect the model parameters in an undesirable way.

4.3.1 Model parameters

When estimating Models A and B, the nonlinear solver was executed until one of two stopping criteria was reached. One of these criteria is the function tolerance which stops the solver if the change in the goal function is smaller than a set value. The second stopping criterion is the step tolerance. This stops the solver if the step size of the solver becomes smaller than a set value. For both criteria the values were set to 10^{-12}. Estimation of the models was repeated several times

Table 4.1: *Thermal parameters for Speaker 1, 2 and 3.*

	$R_0(T_a = 20°C)$	α
Speaker 1	7.7157	0.0033
Speaker 2	6.4007	0.0035
Speaker 3	4.0662	0.0037

Table 4.2: *Signals used for estimation and validation.*

Number	Name	Artist/composer	Type
1	My funny valentine	Bill Evans	Jazz
2	Misty	Ray Bryant	Jazz
3	Morgenstemning	Edvard Hagerup Grieg	Classical
4	Copenaghen steam...	H. C. Lumbye	Classical
5	Our Song	Taylor Swift	Contempory
6	Let em riot	Magnatron	Contempory
7	Dancing in the dark	Bruce Springsteen	Contempory
8	Xmas in Rio	iamMANOLIS	Contempory
9	Doin it right	Daft Punk	Contempory
10	S.H.I.T. advice 2	2kliksphilip	Speech
11	Charlie day almost...	Conan on TBS	Speech
12	Swedlog	Anderzel	Speech

with different initial parameters to minimize the chance of converging to a local minimum. This resulted in the model parameters presented in Table 4.3 The partition function of Model C was estimated using a pink noise signal and N was set to 20 to limit the amount of model parameters. Then the partition function was used when deciding the input to the NARX model. This resulted in the model parameters in Table 4.4.

4.3.2 Case 1: Contemporary music

Songs number 7, 8 and 9 were used for validation for the contemporary music. This gave the results presented in Table 4.5 where $\bar{\epsilon}_{\text{val}} = \frac{1}{n}\sum_{t=1}^{n}|\epsilon|$ denotes the mean absolute error for validation data. Furthermore, $\epsilon_{\max}$ denotes the maximum absolute value of the error ϵ for the validation data and $\bar{\epsilon}_{\text{est}}$ denotes the mean absolute error for estimation data. The simulated outputs for the different models show promising results, see Figure 4.2. However, some characteristics in the data need further discussion. In Figure 4.3, the bias of ϵ is slightly increasing with increasing temperature. However, this increase in bias is rather small and the variance is too large to conclude that there is a trend in the data. The errors for Model A and B, see Figure 4.4, seem to be normally distributed around a positive number. The error of Model C seems not to be normally distributed but rather skewed to the positive side for the contemporary music.

4.3.3 Case 2: Classical music and jazz

Song number 2 and 4 were used for validation for the classical and jazz music. This gave the results presented in Table 4.6. Figure 4.5 shows the main reason for the poor result. Song number 2 seems difficult to predict as all three models have problem coping. Song number 4 had a low error when analysed separately. No good reason has been found for why the result is so different for song number 2 in comparison to all other songs. The only noticeable difference between this song and the others is that the recording is rather noisy.

4.3.4 Case 3: Speech

Song number 10, 11 and 12 were used for validation for the speech case. This gave the results presented in Table 4.7. Figure 4.7 shows the results for song number 10. This is a promising result since the models have not been estimated on speech signals. A common attribute of the speech signals is that the temperature has not been excited to levels above $35°C$. Speech contains many small pauses and therefore the microspeaker is constantly switching between heating and cooling. The histogram of the error, Figure 4.6, shows that the error seems normal distributed around a rather small bias, even for Model C. This has not been true for the other kinds of signals where Model C often has been skewed.

Table 4.3: *Model parameters for Model A and Model B. The model parameters R_1, R_2, C_1, C_2 and ϕ are described in Sections 3.1.1 and 3.1.2.*

	R_1	R_2	C_1	C_2	ϕ
Model A	45.0786	23.6721	0.0448	1.0251	
Model B	47.5992	23.3024	0.0466	1.1803	1.574710^{-6}

Table 4.4: *Model parameters for Model C. The model parameters n_a, n_k, N and a are described in Section 3.2.1.*

	n_a	n_k	N	a
Model C	10	3	20	47.34

Table 4.5: *Model performance for contemporary music.*

	$\bar{\epsilon}_{\text{val}}$	ϵ_{max}	$\bar{\epsilon}_{\text{est}}$
Model A	0.474	1.903	0.138
Model B	0.461	2.152	0.127
Model C	1.076	3.767	0.674

Table 4.6: *Model results for classical music and jazz.*

	$\bar{\epsilon}_{\text{val}}$	ϵ_{max}	$\bar{\epsilon}_{\text{est}}$
Model A	0.8274	3.491	0.319
Model B	0.868	4.542	0.331
Model C	0.8511	4.070	0.613

Table 4.7: *Model results for speech signals.*

	$\bar{\epsilon}_{\text{val}}$	ϵ_{max}
Model A	0.114	0.595
Model B	0.147	1.183
Model C	0.704	2.154

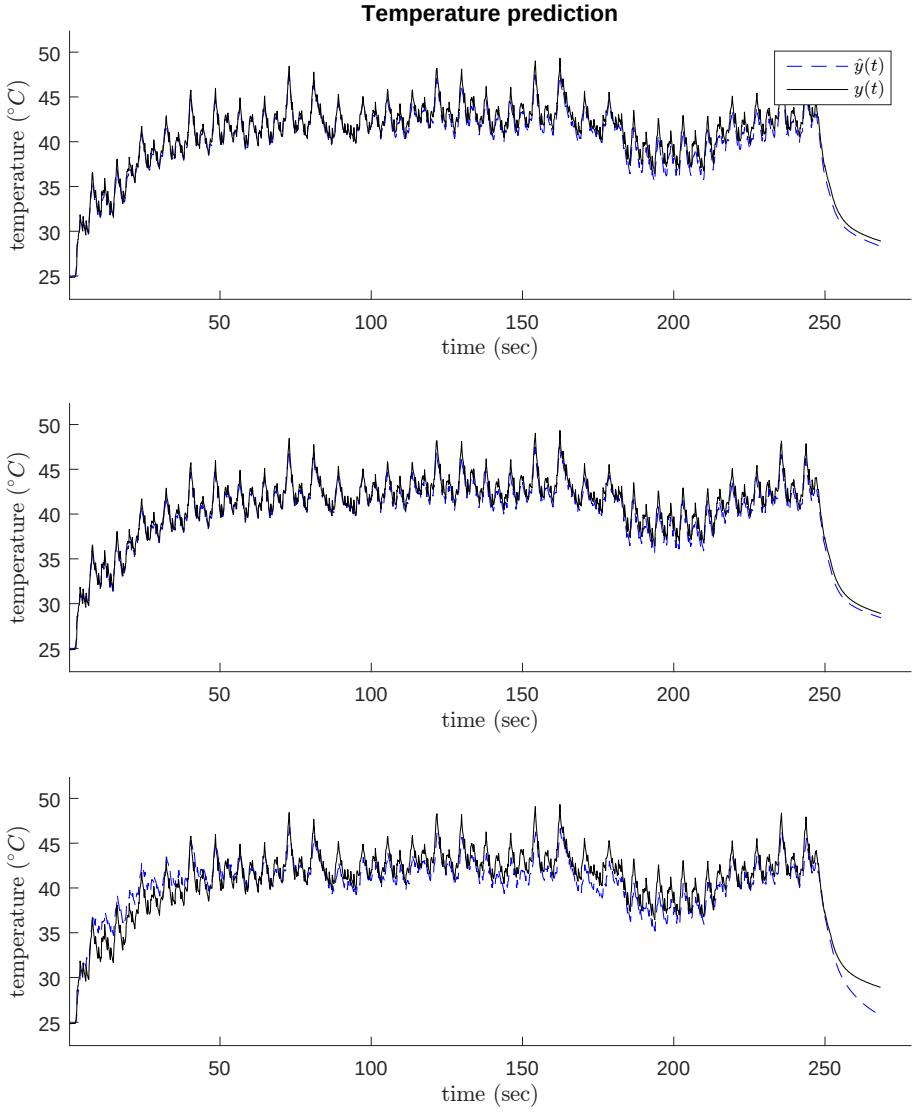

Figure 4.2: *Simulated and measured temperature for Models A (upper), B (middle) and C (lower) for song number 9.*

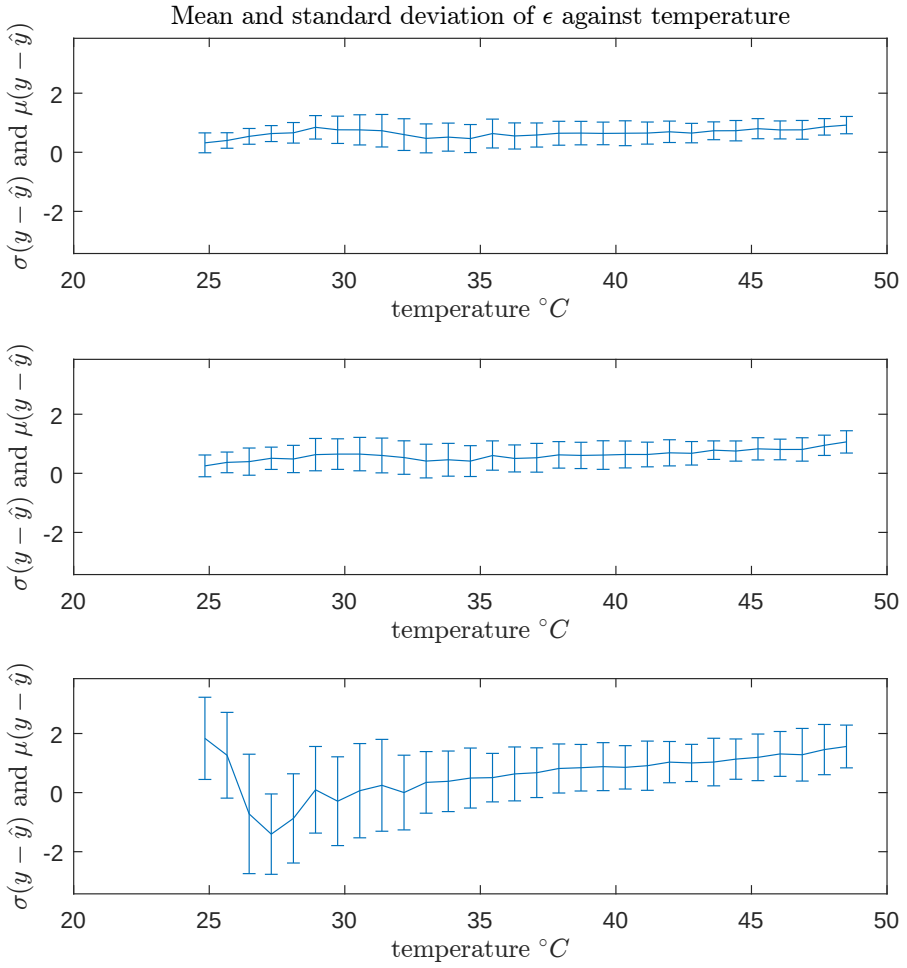

Figure 4.3: *The bias and standard deviation for ϵ for Models A (upper), B (middle) and C (lower) for song number 9 with respect to the temperature.*

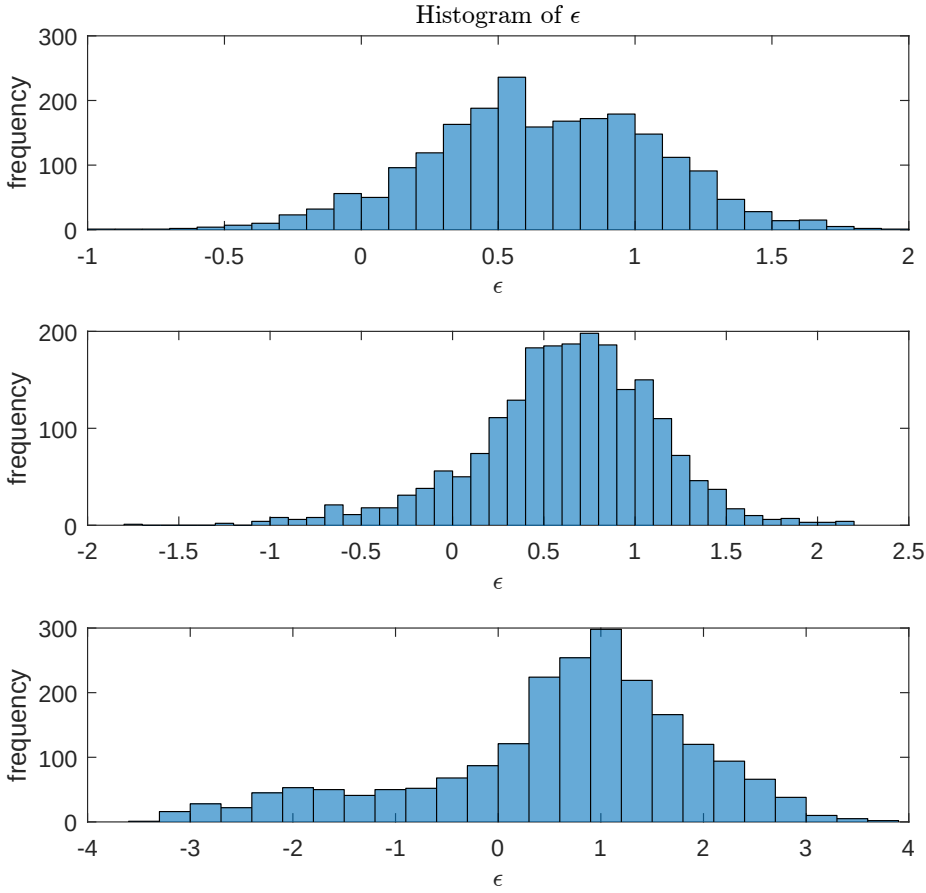

Figure 4.4: *Histogram for the error ϵ for Models A (upper), B (middle) and C (lower) for song number 9.*

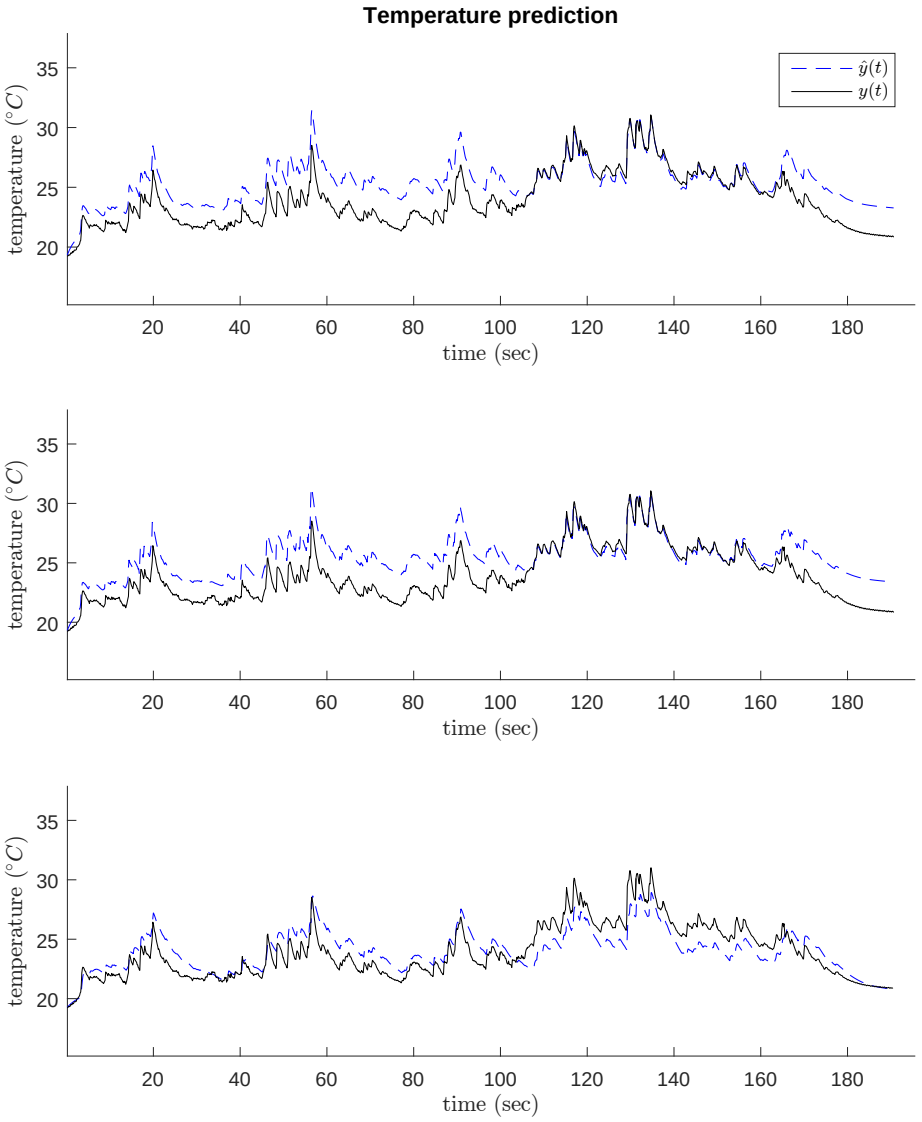

Figure 4.5: *Simulated and measured temperature for Models A (upper), B (middle) and C (lower) for song number 2.*

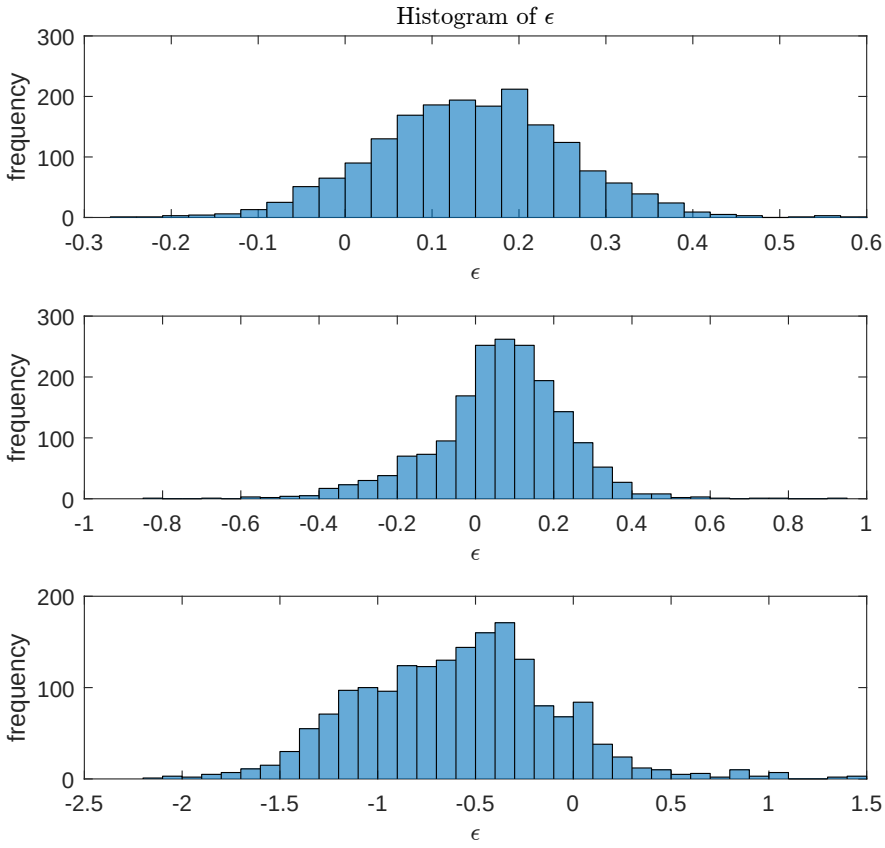

Figure 4.6: *Histogram for the error ϵ for Models A (upper), B (middle) and C (lower) for song number 10.*

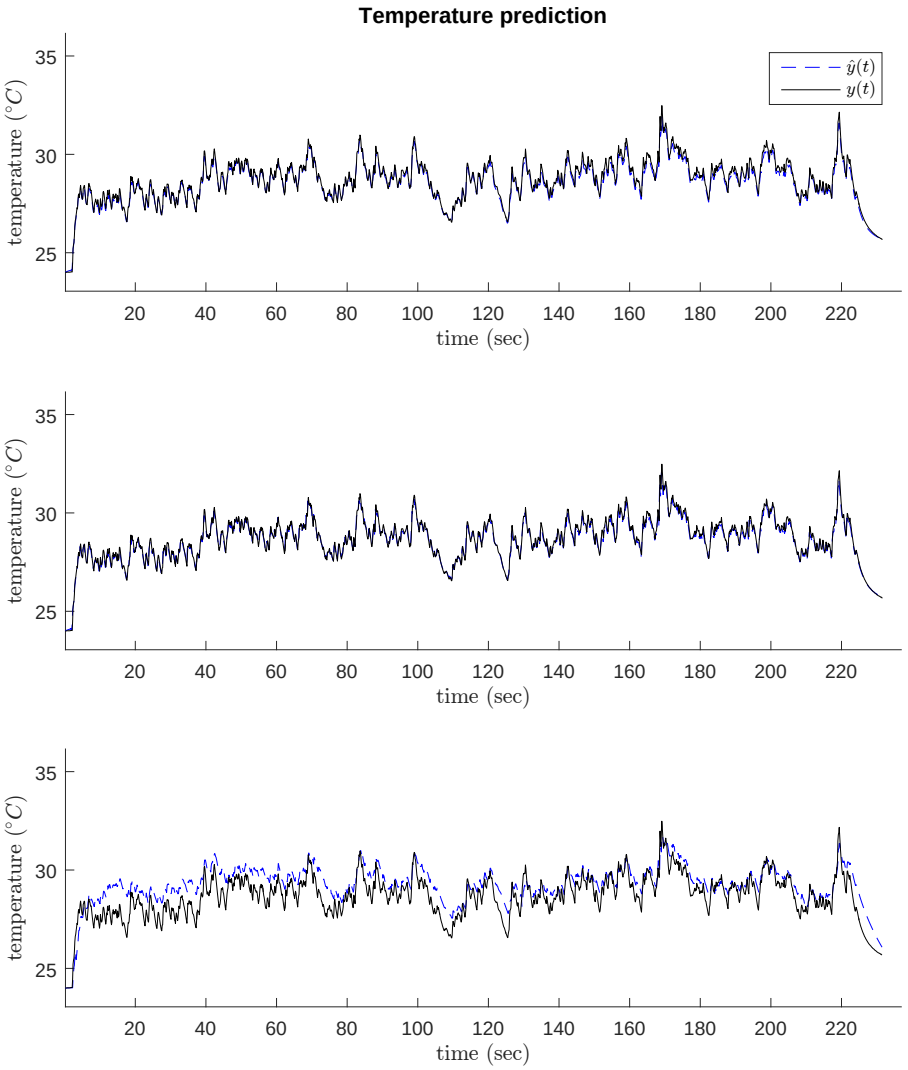

Figure 4.7: *Simulated and measured temperature for Models A (upper), B (middle) and C (lower) for song number 10.*

4.3.5 Comparison of model results

Including all the three cases gives the results shown in Table 4.8. These results show that Models A and B have similar performance and that the results of Model C are slightly worse in comparison. One single song, song number 2, gave the particularly bad maximum error and if this song is excluded from the results the maximum error of Model A and B is lowered to 1.5 and 2.1 , respectively, while model C is still around 4. When comparing Model A and B the difference between the two models is the forced convection parameter in Model B. This seems not to have had any impact on the results. We return to discuss this finding later. The result of Model C must be analysed with the model input taken into account. For example, with increasing temperature the measured current will change according to the power compression factor and affect the input power to Model A and B. The input voltage, however, will stay the same. Therefore, Models A and B are given more information about the system than Model C. That could be one reason why Model C gives slightly worse results than the other two models. In the case of Model A, the performance of the model agrees with the results in Chapman [1998] with the exception of song number 2. Contrary to what have been found here, Model B should give better results than Model A according to Klippel [2004]. We return to discuss this difference later.

4.4 Sensitivity analysis

The sensitivity analysis tests the three models in different scenarios. The stability is tested by changing different parameters one by one and observing the result on the validation data. The model range was tested by changing the ambient temperature around the speaker and observing the model results. Finally, the three models were estimated and implemented for two other speakers, shown in Figure 4.1. This was done to see if the result of the models would vary if implemented on different speakers.

4.4.1 Model parameters

The stability of the three models was tested in two different ways. Model A and Model B were tested by switching the model parameters one by one. The initial parameters were the same as in Section 4.3. For Model A, the parameters R_1, R_2, C_1 and C_2 were shifted with a proportional change from the initial value. The change was made in positive and negative steps of 1, 5, 10, 25, 50 percent from the original value. Since Model B is similar to Model A with the exception of ϕ, only values of ϕ were changed. The result presented is the ratio between the initial and the changed mean absolute error in percentage, calculated as

$$\frac{\bar{\epsilon}_{\text{init}}}{\bar{\epsilon}_{\text{changed}}}, \tag{4.3}$$

where $\bar{\epsilon}_{\text{init}}$ denotes the mean absolute error of the initial parameters and $\bar{\epsilon}_{\text{changed}}$ denotes the mean absolute error for the model with the changed parameters. The

error was calculated for all validation songs. This gave the results in Table 4.9. When comparing the thermal resistance parameters against the thermal capacitance parameters, the former result in a bigger change of the mean error. This is probably because the initial values of R_1 and R_2 are numerically larger than the values of C_1 and C_2 and therefore the overall change of the model is larger. The ϕ parameter gives a better result when the value is reduced. Smaller values of ϕ, gives the forced convection resistance less impact on the model output, showing that the extra parameter in Model B could be unnecessary or badly implemented.

For Model C, the changes to the model were either to model order n_a or the number of partitions N. The result was calculated in the same way as above with the initial values $n_a = 10$ and $N = 20$. The partitions were changed from 8 to 32 and the orders from 5 to 15. The results are presented in Table 4.10. These results indicate that Model C is stable and that small changes to the model parameters do not change the overall performance of the model significantly.

4.4.2 Ambient temperatures

When simulating the different models, the initialisation was done by taking the first observed temperature value and using it as the ambient temperature for the model. This made sure that the model simulation started with the same initial temperature as the observation. The estimation of the model was made at ambient temperatures ranging from 20 to 25 °C. A heat box was used when heating the speaker to different ambient temperatures ranging from 20°C to 50°C with temperature steps of 10°C. At every new ambient temperature song number 6 was played and the voice coil temperature was observed for the loudspeaker. The results for the different ambient temperatures are presented in Table 4.11 when initialising the simulation with the first observed temperature value. The errors are higher than expected and a look at Figure 4.8 shows that the Model A and B underestimates the temperature. It also shows that the initial temperature is not 50°C but 47°C. Therefore the ambient heating of the speaker continues during the playing of the song. This seems to be a problem in most of the ambient temperature test. The expected result was that the model should have overestimated the temperature because of the power compression. This effect was not observed, perhaps because of the problem with the continued ambient heating of the speaker during the playing of the song. Figure 4.9 shows what happens when the model is initialised at room temperature but the ambient temperature is actually higher. As the models simulate the loudspeaker temperature they have no knowledge of the prior temperatures and therefore the initialisation of the model is very important. A bad initialisation will give a bias error for the whole simulation.

4.4.3 Estimating model parameters on different speakers

Different speakers have different thermal properties. For example, the magnet may differ in size or the thickness of the voice coil could lead to a different ther-

Table 4.8: *Model results for all signals.*

	$\bar{\epsilon}_{\text{val}}$	ϵ_{max}	$\bar{\epsilon}_{\text{est}}$
Model A	0.422	3.492	0.234
Model B	0.431	4.542	0.236
Model C	0.882	4.070	0.642

Table 4.9: *Sensitivity analysis on model parameters for Model A and Model B. The result is the ratio between the initial and the changed mean absolute error in percentage.*

Change	$R1$	$C1$	$R2$	$C2$	ϕ
−50%	15	63	28	83	109
−25%	27	89	46	98	105
−10%	50	98	71	101	102
−5%	69	100	84	101	101
−1%	93	100	97	100	100
0%	100	100	100	100	100
1%	107	100	103	100	100
5%	116	99	116	99	99
10%	83	98	124	97	98
25%	34	93	81	91	95
50%	16	83	41	81	90

Table 4.10: *Sensitivity analysis on model parameters for Model C. The result is the ratio between the initial and the changed mean absolute error in percentage. The rows are the change in orders and the columns are the change in partitions.*

orders n_a / partitions	8	14	20	26	32
5	92	92	99	94	93
8	89	98	102	104	97
10	92	101	100	98	92
12	97	99	87	95	85
15	98	112	86	89	94

Table 4.11: *Modelling results for ambient temperature test.*

	$\bar{\epsilon}_{val}$	ϵ_{max}
Model A	2.100	5.566
Model B	2.073	5.648
Model C	2.089	5.912

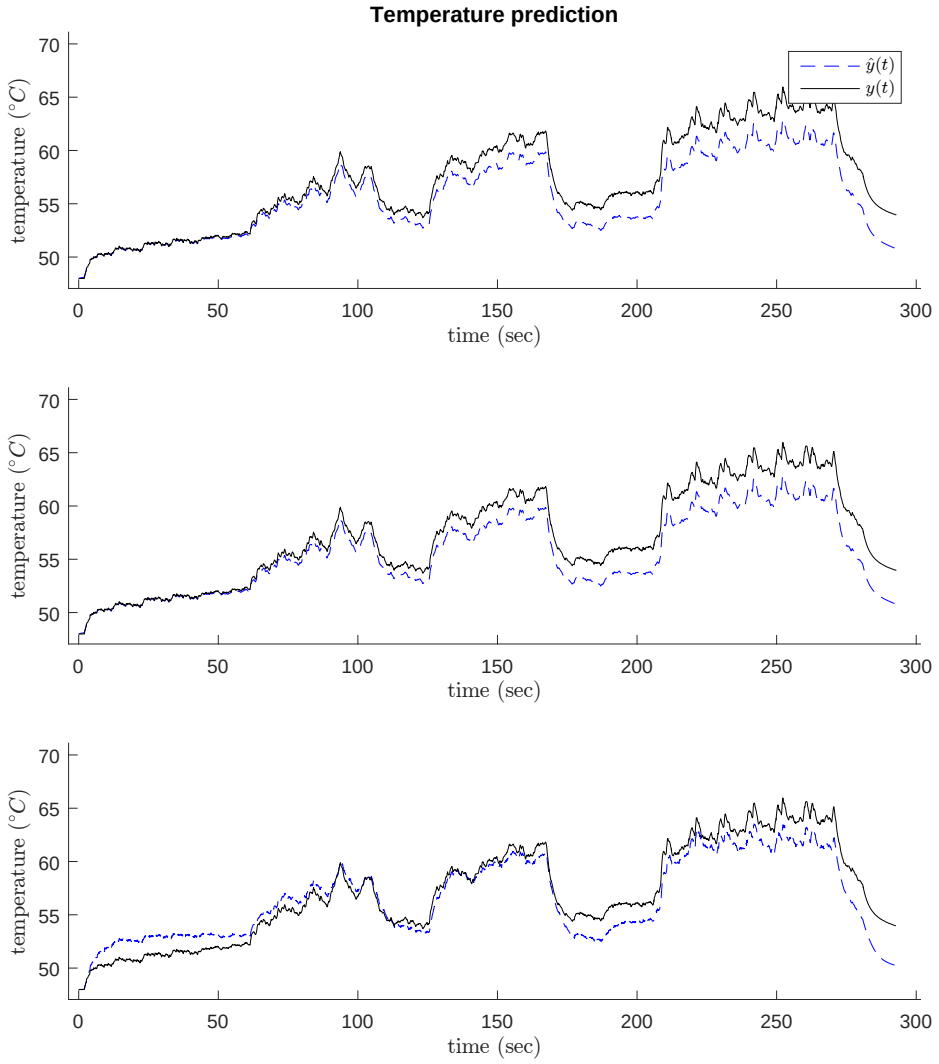

Figure 4.8: *Predicted temperature data for Models A (upper), B (middle) and C (lower) for song number 6 and an ambient temperature of 50 degrees.*

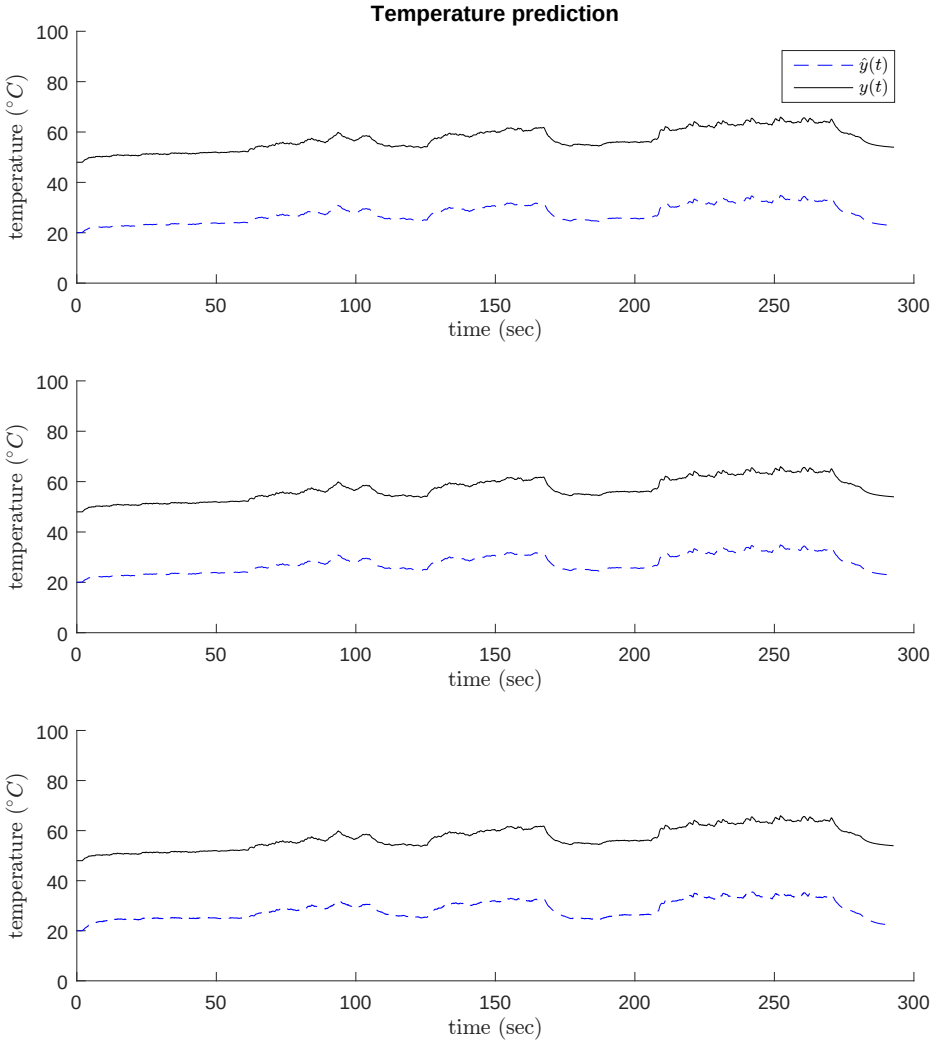

Figure 4.9: *Predicted temperature data for Models A (upper), B (middle) and C (lower) for song number 6 and an ambient temperature of 50 degrees. The model initialization was done at room temperature. This is a rather obvious result considering that the model simulates the system and has no information about the actual temperature. However, the difference between this and Figure 4.8 is important to notice.*

mal behaviour of the speaker. Therefore, the three models have been estimated for two other speakers to find out how easy it is to estimate the model parameters. The estimation of the models was done in the same way as for Speaker 1. One difference from Speaker 1 is that the pilot tone for Speaker 3 is located at 10Hz instead of 40Hz. The validation was done on the same songs as for Speaker 1. This gives the results for Speaker 2 presented in Table 4.12, and the results for Speaker 3 presented in Table 4.13.

The results are promising for Speaker 3 but poor for Speaker 2. This could be due to that the estimation of the model parameters is caught in a local minimum or that the models cannot explain the thermal behaviour of this speaker. Another reason could be the thermal mass of the different speakers. Speaker 2 is similar to Speaker 1 in size whereas Speaker 3 is larger. Hence, it seems that the speaker size is not the reason for the worse performance for Speaker 2. However, Chapman [1998] tried three different sizes of loudspeakers and found that the model accuracy is better when modelling a smaller speaker. This is not observed in this thesis as the best result is observed in the largest speaker. One large difference between Chapman [1998] and this thesis is the input signal used for the estimation. In this thesis ordinary music was used which is a nonstationary signal whereas in the work of Chapman [1998] a pure sine wave signal was used.

4.5 Possible experimental errors

The calibration of the speakers is essential to get correct measurement data. However, the calibration is done by heating up the speaker using a heat box. The heat box itself is supposed to be accurate but no testing was done to ensure this. Even if the heat box is accurate, the time for the speaker to reach the ambient temperature in the speaker is uncertain. This leads to some uncertainty when calibrating the speaker. Here, the speaker was heated for half an hour and it was assumed that the temperature inside the speaker then was the same as the ambient temperature in the heat box.

There is a difficult trade off to consider when using a pilot tone to measure the temperature. The energy of the pilot tone must be sufficiently large so the temperature is measurable but not so large that the result is affected. Hence, the pilot tone level is set to a level that is dependent on the song where the tone is added. Therefore the energy of the pilot tone is different for each song and this gives noisy measurements sometimes.

The velocity signal was calculated from the excursion which was measured using a laser. This measurement was sampled so that the output of an input sine looked like a classical sample and hold output of a sine wave. Efforts were made to fix this by adding a mean average filter. This gave a better but still noisy result. Another mean average filter was applied to the velocity signal to smooth it. This could be a reason why the result of Model B is no better than Model A.

Table 4.12: *Modelling results for Speaker 2.*

	$\bar{\epsilon}_{val}$	ϵ_{max}	$\bar{\epsilon}_{est}$
Model A	1.0074	5.4883	0.6477
Model B	1.0158	5.8531	0.6466
Model C	1.2224	8.0702	1.6771

Table 4.13: *Modelling results for Speaker 3.*

	$\bar{\epsilon}_{val}$	ϵ_{max}	$\bar{\epsilon}_{est}$
Model A	0.2087	1.4383	0.3624
Model B	0.2058	1.3830	0.3615
Model C	0.6027	2.4561	0.3721

5
Conclusions

Model A shows mixed results when simulating the voice coil temperature. The mean error was low, below 0.5°C for Speakers 1 and 3. The maximum error was low, below 2°C with the exception of Speaker 2 and song number 2 for Speaker 1. These are promising results when not considering the exceptions. If the exceptions are considered the results are a bit less promising, especially considering the results from Speaker 2 where the error was higher than expected.

The extra forced convection parameter in Model B does not seem to improve the results. The results are therefore similar to Model A. This could be because of the noisy velocity signal or that the estimation algorithm gets stuck in a local minimum. When estimating Model B, the initial parameters were the estimated parameters from Model A. This could be a reason why the results of Model B are not better than the results from Model A. Chapman [1998] uses a pure sine wave when estimating Model A instead of music that was used in this thesis. When estimating Model A on music the model parameters will be affected by the forced convection effect and adapt to that cool down factor. This would make it difficult for the nonlinear solver to find the optimal solution when trying to fit in the forced convection effect in Model B as it already is accounted for in Model A.

Model C does not give as good results as the grey box models that are considered. However, the results are not fully comparable since the input to Model C is different. Model C has the voltage as input when Model A and B have power calculated from the current. With this in mind, the model gives more promising results. However, when comparing the model complexity against the grey box models there is no good reason why it should be used instead of them.

The sensitivity analysis shows that the models are not parameter sensitive but

that knowing the initial temperature is important for the models to perform well.

The recommendation to Cirrus Logic is to use Model A and to initialise it using a pilot tone that then could be turned off. This would initialise the thermal model in a correct way. If the model starts to predict a dangerously high temperature, the pilot tone could be turned on again and correct the model if there has been a drift of the simulated temperature. This would help with the latency of the feedback and fast temperature changes which has been a problem for Cirrus Logic. It would also use the pilot tone as little as possible. Model A should also be combined with the electromechanical model so the power could be calculated by the latter model. Some longer tests where the temperature reaches higher values are also needed. In this thesis it has not been possible to prove any trends where the variance or the bias has increased over time or temperature. The proposed longer tests can be used to see if this is still correct when the system is exposed with a higher excitation for a longer time period.

Another way would be to assume that only the voltage measurement is available. This would require some temperature data from the mobile device where the microspeaker is installed. If a temperature sensor is present close to the speaker, this could be used to measure the ambient temperature and to initialise the model. This would also need further testing to see if the model is accurate enough and that the initialisation of the model does not introduce a too large error.

The goal of the thesis was to investigate if a feed-forward thermal model could be used to simulate the voice coil temperature. The results indicate that this is indeed possible if the model is initialised at the correct temperature. Model A performs best out of the three models and it seems that two RC-components are sufficient for microspeakers which are not installed in a device. If installed in a device, three RC-components could be needed to model the extra thermal mass.

Bibliography

R. Andersson. Loudspeaker voice-coil temperature estimation. MSc thesis, Luleå University of Technology, 2008. Cited on pages 2 and 3.

G. K. Behler and A. Bernhard. Measuring method to derive the lumped elements of the loudspeaker thermal equivalent circuit. In Proceedings of *Audio Engineering Society Convention 104*, Amsterdam, Netherlands, May 1998. Cited on pages 3 and 8.

F. Blasizzo. A new thermal model for loudspeakers. *Journal of the Audio Engineering Society*, 52(1/2):43–56, 2004. Cited on page 4.

A. Bright. Active control of loudspeakers: An investigation of practical applications. PhD thesis, Technical University of Denmark, 2002. Cited on page 7.

D. J. Button. Heat dissipation and power compression in loudspeakers. *Journal of the Audio Engineering Society*, 40(1/2):32–41, 1992. Cited on pages 3, 7, 16, and 17.

P. J. Chapman. Thermal simulation of loudspeakers. In Proceedings of *Audio Engineering Society Convention 104*, Amsterdam, Netherlands, May 1998. Cited on pages 3, 4, 11, 15, 16, 17, 18, 37, 42, and 45.

C. A. Henricksen. Heat transfer mechanisms in loudspeakers; analysis, measurement and design. In Proceedings of *Audio Engineering Society Convention 80*, Montreux, Switzerland, Mar 1986. Cited on pages 3, 7, 8, 9, 15, 16, and 17.

W. Klippel. Nonlinear modeling of the heat transfer in loudspeakers. *Journal of the Audio Engineering Society*, 52(1/2):3–25, 2004. Cited on pages 2, 4, 8, 9, 11, 18, and 37.

L. Ljung and T. Glad. *Modellbygge och Simulering*. Studentlitteratur Lund, second edition, 2004. Cited on pages 15 and 19.

Marketline. *Mobile Phones Industry Profile: Global*, pages 1–37, 2015. Cited on page 1.

B. Pedersen and P. Rubak. Musical transducer-less indentification of linear loudspeaker parameters. In Proceedings of *the 32nd International Conference of the Audio Engineering Society*, pages 75–82, Copenhagen, Denmark, Sep 2007. Cited on page 2.

Polyfit function. `http://se.mathworks.com/help/matlab/ref/polyfit.html/`. Online; accessed 12-Jun-2016. Cited on page 25.

R. H. Small. Closed-box loudspeaker systems Part 1: Analysis. *Journal of the Audio Engineering Society*, 20(10):798–808, 1972. Cited on page 2.

N. Thiele. Loudspeakers in vented boxes: Part 1. *Journal of the Audio Engineering Society*, 19(5):382–392, 1971. Cited on page 2.

C. Zuccatti. Thermal parameters and power ratings of loudspeakers. *Journal of the Audio Engineering Society*, 38(1/2):34–39, 1990. Cited on pages 3, 8, 16, and 17.

Appendix

A

Equipment and experimental setup

The experimental setup measures the voltage and the current over the speaker. The excursion is also measured using a laser. The experimental setup can be seen in Figure A.2. The equipment used for the experimental setup was:

- An ART SLA-1, 100 Watt amplifier.
- A NI USB-4431, 24-bit I/O-device with four analog input channels and one analog output channel.
- A measurement circuit board for measuring the current and voltage over the speaker.
- Several AAC-A micro speakers.
- A VT 4002, Vötsch Industrietechnik, heatbox with ±0.3°C sensitivity.
- A Keyence LK-G37 laser.

Using the I/O device, a signal is sent to the amplifier, which is connected to the measurement circuit board which in turn is connected to the speaker. From the circuit board, the voltage and the current is measured and connected to the I/O device. The laser is also connected to this device. Using this setup, measurements have been collected with a sampling frequency up to 48kHz. The heatbox was used when calibrating the pilot tone. A pilot tone with low voltage was run through the speaker and the resistance of the speaker was measured for different temperatures.

Figure A.1: *The experimental setup used in this thesis. The speaker is situated on the left and measured by the laser. The amplifier and the circuit board is situated in the middle. The I/O device and the computer that collects the measurements can be seen to the right.*

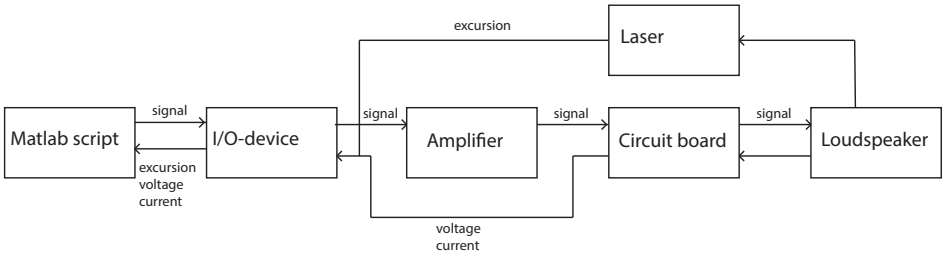

Figure A.2: *A block scheme for the experimental setup and how the different equipment interacts with each other.*